Extraction of Complex Permittivity and Permeability in a Coaxial TEM-Chamber Using a Multilayer Perceptron

Ilya A. Ivantsov
Scientific Research Laboratory
of Basic Research
on Electromagnetic Compatibility
Tomsk State University of Control Systems
and Radioelectronics
Tomsk, Russia
wertygo123@outlook.com

Nikita V. Pavlov
Scientific Research Laboratory
of Basic Research
on Electromagnetic Compatibility
Tomsk State University of Control Systems
and Radioelectronics
Tomsk, Russia
nikita.s.pavlov@tusur.ru

Yuri V. Kalashnikov
Scientific Research Laboratory
of Basic Research
on Electromagnetic Compatibility
Tomsk State University of Control Systems
and Radioelectronics
Tomsk, Russia
yurakalashnikov2002@outlook.com

Valery A. Semenyuk
Scientific Research Laboratory
of Basic Research
on Electromagnetic Compatibility
Tomsk State University of Control Systems
and Radioelectronics
Tomsk, Russia
semenyuk_va@tu.tusur.ru

Yevgeniy S. Zhechev
Scientific Research Laboratory
of Basic Research
on Electromagnetic Compatibility
Tomsk State University of Control Systems
and Radioelectronics
Tomsk, Russia
zhechev75@gmail.com

***Abstract*—This paper proposes an approach for extracting complex permittivity and permeability using a measurement setup based on a coaxial TEM chamber and a multilayer perceptron (MLP). The approach accounts for the thickness and longitudinal displacement of the sample. A training database was generated via full-wave finite element method (FEM) simulations in the 0.1–3 GHz range. Data preprocessing was applied to filter out non-physical numerical artifacts and enforce passivity conditions. The MLP model was trained using a physics-constrained loss function. Validation results demonstrated a Mean Absolute Error (MAE) of $6.98 \cdot 10^{-3}$ and an R^2 of 0.999. Verification on a simulated samples showed that the maximum relative error across the reconstructed parameters (ε', μ', ε'', μ'') did not exceed 3.24% within the specified frequency band.**

Keywords*—Complex permittivity and permeability, coaxial TEM cell, inverse scattering problem, microwave measurements, multilayer perceptron, physics-constrained machine learning.

I. Introduction

Extraction of complex permittivity and permeability is a key task in electrodynamics, necessary for calculating the characteristics of radio frequency devices, antennas, and composite materials, as these parameters directly determine the propagation, reflection, and absorption of electromagnetic waves in a medium [1, 2]. Currently, a significant number of methods have been developed for measuring the electromagnetic parameters of materials in the microwave range, which can be classified into waveguide, resonator, and probe approaches. The most common methods are based on measuring the complex scattering parameters of two-port structures, including the classic Nicolson-Ross-Weir (NRW) method, which recovers the permittivity and permeability from the reflection and transmission coefficients of a sample in a waveguide or coaxial line [3, 4]. In addition, resonator methods based on analyzing frequency shifts and changes in quality factor are widely used [6, 7], as well as open-ended coaxial probe methods for rapid diagnostics of liquids and tissues [8], and free-space methods for large-scale or anisotropic structures with a plane-wave illumination of the sample [9, 10]. These approaches are regulated by standards (e.g., ASTM D5568 for waveguide measurements) and provide frequency-dependent complex parameters in laboratory and industrial settings [11, 12].

However, existing methods have several drawbacks that limit their applicability. Transmission and reflection coefficient-based methods (NRW) only work correctly when the sample perfectly fills the regular cross-section of the transmission line, while resonator-based methods are limited to a discrete set of eigenfrequencies of the resonant cavity [4–7]. A significant number of algorithms exhibit instability when measuring materials with magnetic losses or large electrical thickness due to phase ambiguity and singularities in the solutions [3, 13]. Free-space methods require complex anechoic equipment and precision antennas, and to eliminate air gaps in coaxial and strip cells, the sample must be conformable or powdered [9, 10, 14].

In this study, we utilize a measurement setup based on a coaxial TEM-chamber with a longitudinally non-uniform cross-section. While a transition from the calibration planes to the sample planes can be performed using an analytical solution [15], deriving such a solution for this specific chamber geometry presents significant complexity. In such cases, stochastic algorithms offer a more feasible alternative for extracting material parameters from the frequency dependencies of the scattering parameters. These include linear or polynomial regression, decision trees, and random forest. Furthermore, the application of machine learning, in particular artificial neural networks (ANNs), is a relevant solution [16, 17]. As demonstrated in [18], ANNs can outperform the aforementioned algorithms (linear/polynomial regression, decision trees, random forest) in terms of accuracy and robustness for transmission line problems, owing to their ability to approximate complex nonlinear dependencies. Consequently, neural networks are effective for reconstructing the electromagnetic parameters of materials from S-parameters, typically using a training set generated from numerical simulations of the system for different material property values [16, 17, 19].

The primary objective of this paper is to propose and validate a method for extracting the electromagnetic parameters of materials using a coaxial TEM-chamber. The proposed approach is specifically intended to enable the measurement of magnetic materials with small sample sizes over a wide frequency range.

II. Simulation and Extraction Approach

Solving this problem using artificial neural networks involves data collection and model training. The data collection was performed using full-wave simulation. The simulation results were processed to remove errors and non-physical results, and data normalization was also performed. Next, the model was configured and trained. To evaluate the quality of model training, the MAE and R^2 values were calculated.

A. *TEM-chamber, sample and simulation*

The geometric model of the TEM-chamber is a coaxial two-port measurement system with smooth conical transitions designed to match the working area with a characteristic impedance of 50 ohms at the input and output ports. The inner conductor has a diameter of $d_1 = 20$ mm, and the outer conductor has a diameter of $d_2 = 44.88$ mm. The design includes a cylindrical working area for the sample placement and matching transitions to standard coaxial SMA connectors for connection to a vector network analyzer. The length of the working part of the chamber is selected based on the need to create a fundamental TEM mode in the studied frequency range and to suppress the excitation of higher-order modes. The sample is modeled as an annular material under test (MUT), whose parameters are determined by its length (l), inner and outer diameters (d_1 and d_2), and longitudinal shift relative to the center of the chamber (b). Full-wave modeling using the finite element method (FEM) was performed to collect the database in the range from 0.1 to 3 GHz.

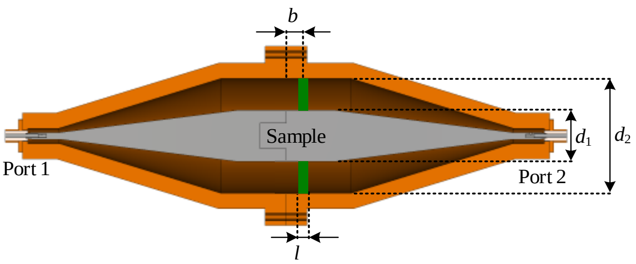

Fig. 1. Longitudinal section of a TEM-chamber coaxial line with a MUT.

B. *Data Base Compilation Approach*

To ensure the reliability of the simulated *S*-parameters and improve the accuracy of the neural network's approximation of electromagnetic parameters, preliminary filtering of the compiled database was performed. This allowed for the exclusion of non-physical results and numerical artifacts. The processing begins with a verification of the fundamental principle of passivity of the electrodynamic system by analyzing the magnitudes of the scattering coefficients. The magnitude values of the *S*-parameters across the entire studied frequency range must strictly satisfy the condition $0 \le |S_{ij}| \le 1$. Furthermore, the Lorentz reciprocity theorem implies the equality of S_{12} and S_{21}. For this purpose, the relative deviation between them must not exceed 10^{-3}:

$$\frac{|S_{12} - S_{21}|}{0.5\left(|S_{12}| + |S_{21}|\right)} \le 10^{-3} . \quad (1)$$

The database was also cleansed of sharp jumps and local anomalies in the frequency responses of *S*-parameters caused by errors in full-wave simulation. To achieve this, a condition was developed according to which the derivative of the function $20 \times \log(|S_{ij}|)$ must not change sign more than n times over a sliding interval of m points. The sign of the derivative is determined according to:

$$\sigma_i = \operatorname{sign}(g_i) = \begin{cases} 1, & \text{if } \sigma_i > 0 \\ 0, & \text{if } \sigma_i = 0 \\ -1, & \text{if } \sigma_i < 0 \end{cases} . \quad (2)$$

For each interval of length m starting at index k ($1 \le k \le N - m + 1$), the number of sign changes of the derivative can be defined as:

$$C_k = \sum_{i=k}^{k+m-2} 1\{\sigma_i \ne 0, \sigma_{i+1} \ne 0, \sigma_i \ne \sigma_{i+1}\} , \quad (3)$$

where 1{} is the indicator function, which equals 1 if the condition is true and 0 otherwise.

Subsequently, a Boolean variable is calculated to indicate whether the rows should be removed from the database:

$$h_i = \prod_{k=\max(1,\, i-m+1)}^{\min(i,\, N-m+1)} 1\{C_k \le n\} . \quad (4)$$

If, during the analysis of a database row, non-compliance with the conditions was detected, the row was classified as incorrect and subject to removal from the database array.

Since the measurement setup under consideration is passive, the reciprocity condition holds for it: equality of the transmission coefficients S_{12} and S_{21}. Thus, only the transmission coefficient S_{12} was retained in the final database. The resulting array was divided into an input feature array and a target parameter array. The input feature array has dimensions (N, 9) and includes frequency, Re(S_{11}), Im(S_{11}), Re(S_{21}), Im(S_{21}), Re(S_{22}), Im(S_{22}), l, and b. The target parameter array has dimensions (N, 4) and includes ε′, ε″, μ′, and μ″. The parameter variation ranges are shown in Table I and were selected based on the characteristics of typical composite and magnetodielectric materials.

The total size of the training sample N is determined as the product of the discrete values of all varied parameters. With a typical frequency grid, the total data volume exceeds $9 \cdot 10^6$ entries, which guarantees sufficient coverage density of the parameter space to minimize the approximation error.

TABLE I. PARAMETERS RANGES AND NUMBER OF POINTS

Parameter	Range/Values	Number of points
f (GHz)	0.1 – 3	1001
ε′	1; 2.1; 4.3; 10; 20; 23	6
ε″	0.00042; 0.05; 0.1075; 2; 5	5
μ′	1; 2; 3; 4; 5	5
μ″	0.00001; 0.001; 0.1; 1.2; 2	5
l (mm)	0.5; 1; 2	3
b (mm)	0; 0.25; 0.5; 1	4

Total DB size: 9 009 000

Data preprocessing includes the normalization of input features and target values to the interval [0, 1] using the linear scaling method, in which the normalized value is determined based on the minimum ($x_{\min}$) and maximum ($x_{\max}$) values of the corresponding feature in the training set:

$$x_{\text{norm}} = \frac{x - x_{\min}}{x_{\max} - x_{\min}}. \quad (5)$$

The generated database was randomly divided into training, validation, and test subsets in a ratio of 80/10/10.

C. ANN Model Structure

In this work, we used a multilayer perceptron (MLP) as a sequential fully connected neural network, which consists of an input layer with 9 neurons corresponding to the input parameters, 5 hidden layers with 128 neurons each, and an output layer with 4 neurons that predict the real and imaginary parts of the complex permittivity and permeability. The ReLU (Rectified Linear Unit) activation function is used in the hidden layers, defined as ReLU(x)=max(0, x), which converts negative values to zero while leaving positive values unchanged. The MLP architecture is shown in Fig. 2.

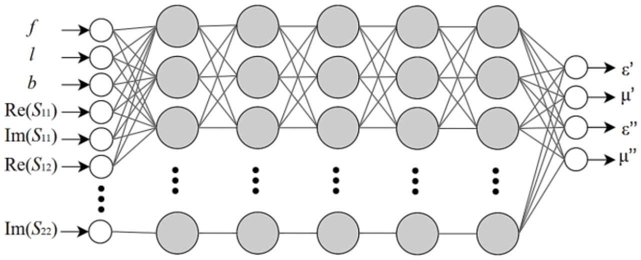

Fig. 2. Architecture of MLP.

The neural network was trained for 200 epochs using a modified mean squared error (MSE) function, which additionally takes into account physical constraints on the predicted parameters, such as the minimum values of the real parts of the complex permittivity and permeability and the non-negativity of their imaginary parts (6). The neural network was trained on an Intel Core i9-13900KF CPU with DDR5 6000 MHz RAM, and the total training time was 45 minutes and 26 seconds. The figure shows the graphs of the change in the mean absolute error (MAE) and the coefficient of determination (R^2) as a function of the number of training epochs. The graphs demonstrate that the model achieves a low error on the training set, while the error on the validation set does not exceed the error on the training set, indicating stable training without signs of overfitting. In (6) y' is the predicted values of the neural network, y is the true values of the target parameters from the database, and λ_{phys} is the physical penalty coefficient that sets the weight of the additional constraint on the predicted parameters (in this work, $\lambda_{\text{phys}} = 10^{-2}$).

Fig. 3 shows the dependence of MAE and the coefficient of determination R^2 on the number of epochs for training and validation samples. The graphs show that MAE tends to zero, and the coefficient of determination tends to 1, which means that 200 epochs is enough for high-quality training of the model. Also, the error during training does not exceed the error during validation, which means that retraining is not observed.

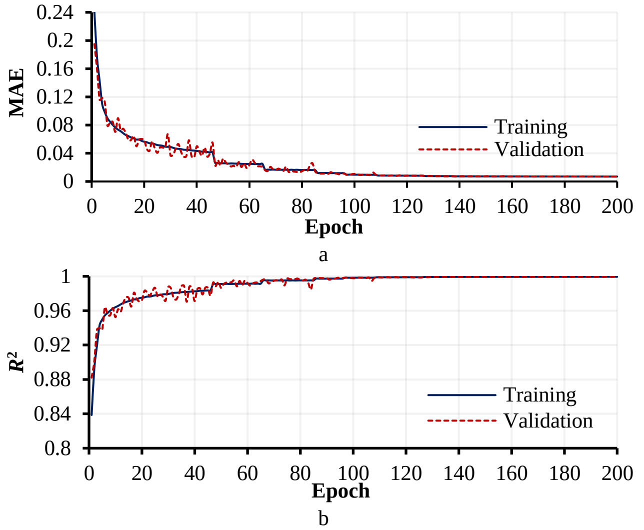

Fig. 3. Dependencies of MAE and R^2 on the number of epochs: training (▬), validation (▪▪▪).

III. RESULTS

Fig. 4, 5, and 6 show the frequency dependencies of ε′, ε″, μ′, and μ″ obtained from the reference and the trained model for PTFE, FR4, and magnetic material with l =1 mm, b = 0 and b = 1.

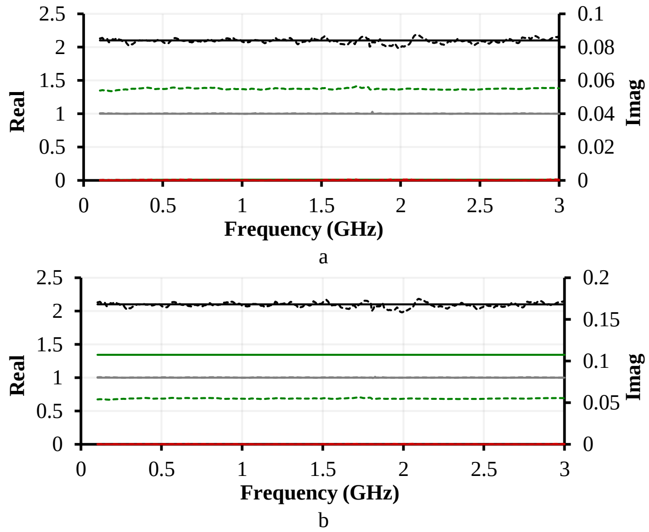

Fig. 4. Frequency dependencies of reference ε′ (▬), ε″ (▬), μ′ (▬), and μ″ (▬) and trained model ε′ (▪▪▪), ε″ (▪▪▪), μ′ (▪▪▪), and μ″ (▪▪▪) for PTFE with b = 0 (a) and b = 1 mm (b)

$$F_{loss} = \frac{1}{4}\sum_{i=1}^{4}\left(y_i - y'_i\right)^2 + \lambda_{phys}\left[\mathrm{ReLU}(1-\varepsilon') + \mathrm{ReLU}(-\varepsilon'') + \mathrm{ReLU}(1-\mu') + \mathrm{ReLU}(-\mu'')\right]. \quad (6)$$

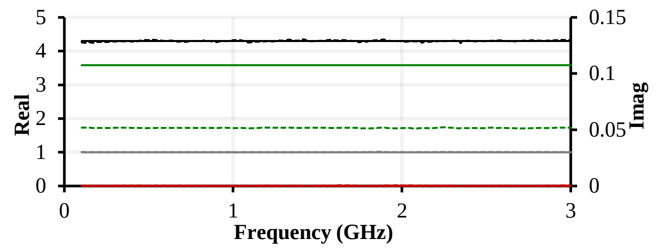

a

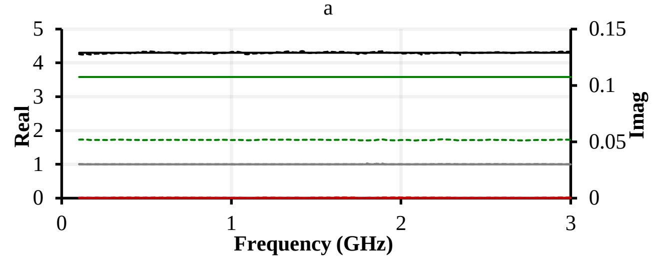

b

Fig. 5. Frequency dependencies of reference ε′ (▬), ε″ (▬), μ′ (▬), and μ″ (▬) and trained model ε′ (▪▪▪), ε″ (▪▪▪), μ′ (▪▪▪), and μ″ (▪▪▪) for FR4 with b = 0 (a) and b = 1 mm (b)

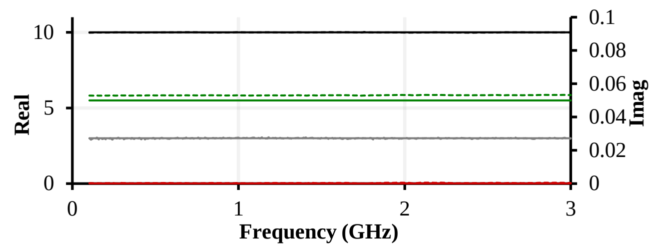

a

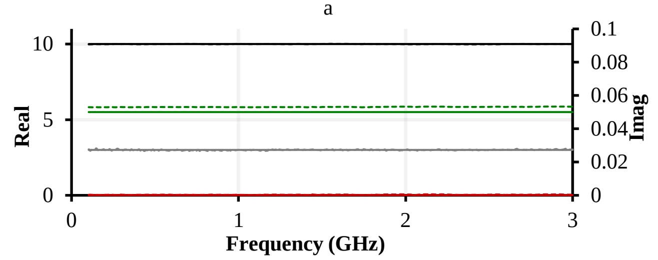

b

Fig. 6. Frequency dependencies of reference ε′ (▬), ε″ (▬), μ′ (▬), and μ″ (▬) and trained model ε′ (▪▪▪), ε″ (▪▪▪), μ′ (▪▪▪), and μ″ (▪▪▪) for magnetic material with b = 0 mm (a) and b = 1 mm (b)

The tab. II shows the root mean square errors of ε′, ε″, μ′, and μ″ for FR4, PTFE, and the magnetic material without shift and with sample displacement in the TEM chamber.

TABLE II. RMS ERRORS OF OBTAINED PERMITTIVITY AND PERMEABILITY

Materials	RMS Errors				
	ε′	ε″	μ′	μ″	Full
PTFE	0.035	0.053	0.004	$3.1\cdot10^{-4}$	0.032
FR4	0.019	0.055	0.005	$4.1\cdot10^{-4}$	0.029
Magnetic Sample	0.008	0.003	0.027	$2.6\cdot10^{-4}$	0.014
PTFE (shifted)	0.038	0.052	0.004	$3\cdot10^{-4}$	0.031
FR4 (shifted)	0.019	0.055	0.005	$5.4\cdot10^{-4}$	0.029
Magnetic Sample (shifted)	0.008	0.003	0.026	$2.6\cdot10^{-4}$	0.013

IV. CONCLUSION

The paper demonstrates the extraction of complex permittivity and permeability of materials using an artificial neural network model applied to a measuring chamber with an irregular cross-section. To solve the problem, a database was created using full-wave modeling. The data was preprocessed, including filtering out modeling artifacts (eliminating sharp jumps and non-physical results that violate the passivity condition), as well as normalizing the features to a range of 0 to 1. The artificial neural network model was trained using the TensorFlow framework in Python. The network architecture consisted of an input layer with 9 neurons (corresponding to the values of S_{11}, S_{12}, S_{22}, frequency, length, and shift of the sample), an output layer with 4 neurons (complex ε and μ), and 5 hidden fully connected layers with 128 neurons each. The training process took 200 epochs and 45 minutes and 26 seconds. The ReLU activation function was used. The effectiveness of the proposed approach was evaluated using a test set. Verification on a simulated samples showed that the maximum relative error across the reconstructed parameters (ε', μ', ε", μ") did not exceed 3.24 % within the specified frequency band.

Despite the achieved accuracy, the method has a number of limitations. Firstly, when changing the measurement chamber, it is necessary to re-collect the training sample and retrain the model, which in turn requires a precision model of the chamber in the full-wave electrodynamic simulation environment. Secondly, the trained model's applicability is limited to the ranges of input parameters (sample geometry, frequency range, and ε and μ values) contained in the training sample. Going beyond these limits leads to incorrect algorithm operation, requiring the expansion of the database. The key current drawback is the significant error of the method when applied to real experimental data. To overcome this limitation, it is planned to implement a fine-tuning procedure for the model based on the results of field measurements. It is planned to use samples with known electromagnetic parameters as reference samples, and to conduct measurements in a coaxial TEM-chamber using a vector network analyzer.

It is worth noting that the proposed approach, based on the behavioral MLP model, is empirical and the easiest to implement for measuring chambers with complex geometry. At the same time, the problem has a potential analytical solution, which requires transferring the calibration planes directly to the sample planes for subsequent application of classical algorithms (NRW, NIST iterative method). In the future, the results of this work can be used as the basis for a standard methodology for extracting electromagnetic parameters, where the user creates a database in a full-wave modeling system and then uses unified software tools (pre-prepared MLP processing and training scripts) to synthesize a model suitable for subsequent application to experimental S-parameters. This approach can be recommended for measuring chambers with arbitrary geometry, where analytical methods for solving the inverse problem are difficult to implement or non-existent.

ACKNOWLEDGMENT

The research was funded by the Ministry of Science and Higher Education of the Russian Federation, project FEWM 2024-0005.

REFERENCES

[1] J. Obrzut. Measurement of Materials Dielectric Properties. National Institute of Standards and Technology (NIST), 2006.

[2] C. A. Balanis. Advanced Engineering Electromagnetics. Wiley, 2012.

[3] Nicolson, A. M. and G. F. Ross, "Measurement of the intrinsic properties of materials by timedomain techniques," IEEE Trans. Instrum. Meas., vol. 19, No. 4, 377–382, 1970.

[4] W. B. Weir. “Automatic measurement of complex dielectric constant and permeability at microwave frequencies.” IEEE Transactions on Microwave Theory and Techniques, 1974, vol. 22, No. 1, pp. 33–36

[5] L. Chen, C. K. Ong, C. P. Neo, V. V. Varadan, and V. K. Varadan, Microwave Electronics: Measurement and Materials Characterization. Hoboken, NJ, USA: Wiley, 2004.

[6] M. N. Afsar, J. R. Birch, and R. N. Clarke, "The measurement of the properties of materials," Proc. IEEE, vol. 74, no. 1, pp. 183–199, Jan. 1986.

[7] M. B. Barmatz, H. W. Jackson, A. S. Javeed, C. S. Jamieson, and D. E. Steinfeld, "An Accurate Radially Stratified Approach for Determining the Complex Permittivity of Liquids in a Cylindrical Microwave Cavity," IEEE Trans. Microw. Theory Techn., vol. 63, no. 2, pp. 504–508, Feb. 2015.

[8] J. Baker-Jarvis, M. D. Janezic, P. D. Domich, and R. G. Geyer, "Analysis of an open-ended coaxial probe with lift-off for nondestructive testing," IEEE Trans. Instrum. Meas., vol. 43, no. 5, pp. 711–718, Oct. 1994.

[9] A. A. Belyaev, A. M. Romanov, V. V. Shirokov, and E. M. Shuldeshov, "Measurement of honeycomb glass fiber plastics permittivity in free space," Trudy VIAM, no. 5, May 2014.

[10] N. A. Pevneva, D. A. Kondrashov, A. L. Gurskii, and A. V. Gusinsky, "Estimation of S-parameters and dielectric permittivity of quartz ceramics samples in millimeter waveband," Doklady BGUIR, vol. 19, no. 7, pp. 65–71, 2021.

[11] ASTM D5568-22a, "Standard Test Method for Measuring Relative Complex Permittivity and Relative Magnetic Permeability of Solid Materials at Microwave Frequencies Using Waveguide," ASTM International, West Conshohocken, PA, 2022.

[12] IEEE Std 1309-2013. “IEEE Standard for Calibration of Electromagnetic Field Sensors and Probes.”

[13] T. L. Blakney, "Comments on 'Automatic measurement of complex dielectric constant and permeability at microwave frequencies'," Proc. IEEE, vol. 63, no. 1, pp. 203–205, Jan. 1975.

[14] D. S. Klygach, M. G. Vakhitov, D. G. Fomin, and A. S. Korolev, "A device for measuring the dielectric properties of powder materials based on a stripline transmission," Bull. South Ural State Univ. Ser. Comput. Technol. Autom. Control Radio Electron., vol. 22, no. 4, pp. 159–166, 2022.

[15] ASTM ES7–1983. Test method for electromagnetic shielding effectiveness of planar materials.

[16] Q. J. Zhang, K. C. Gupta. Neural Networks for RF and Microwave Design. Artech House, 2000.

[17] C. Christodoulou, M. Georgiopoulos. Applications of Neural Networks in Electromagnetics. Artech House, 2001.

[18] Pavlov, N. S., and Y. S. Zhechev. "Comparison of Machine Learning Regression Models for Coupled Microstrip Line Parameter Synthesis." *Mathematical Models and Computer Simulations* 16.Suppl 1 (2024): S96-S104.

[19] H. Li, J. Li, Y. Long. Accuracy-Improved and Low-Cost Material Characterization Using Power Measurement and Artificial Neural Network. IEEE Access, 2020.